Faculty of Pharmaceutical Sciences[1], Setsunan University, Osaka; Thinky Corporation[2], Tokyo, Japan

Scaling up nano-milling of poorly water soluble compounds using a rotation/revolution pulverizer

K. Yuminoki[1], S. Tachibana[1], Y. Nishimura[1], H. Mori[1], T. Takatsuka[2], N. Hashimoto[1]

Received May 28, 2015, accepted August 10, 2015

Kayo Yuminoki, Faculty of Pharmaceutical Sciences, Setsunan University, 45-1 Nagaotoge-cho, Hirakata, Osaka 573-0101, Japan
yuminoki@pharm.setsunan.ac.jp

Pharmazie 71: 56–64 (2016) *doi: 10.1691/ph.2016.5093*

We previously reported that a rotation/revolution pulverizer (NP-100) could mill a small amount of a drug (0.1 g) into nanoparticles in several minutes. In this investigation, scale up from the milligram to the kilogram scale of the nano-milling process by the rotation/revolution pulverizer was studied. Phenytoin was used as a model drug with low solubility in water. After confirming the improvement of the phenytoin bioavailability by milling to nanoparticles using NP-100, scaling parameters were evaluated using NP-100 and the middle scale model of NP-100 (ARV-3000T). A theoretical equation for the specific collisional energy was adapted for wet milling; this suggested that the relative centrifugal acceleration of revolution (revolution G) and the drug concentration in the suspension were the two most important parameters. The results obtained using NP-100 and ARV-3000T correlated well when these two parameters were identical. These results were applied to the large scale model of NP-100 (ARV-10KT), where 2 kg (1 kg × 2) of phenytoin nanoparticles were obtained in 60 min. The results from PXRD and DSC indicated that the milled phenytoin by ARV-3000T and ARV-10KT maintained its crystallinity. These results suggest nano-milling using a rotation/revolution pulverizer will be widely applicable to the development of nano-medicine.

1. Introduction

Advances in combinatorial chemistry and high-throughput screening have resulted in an increase in the number of drug candidates with high pharmacological activity currently in development. However, most of these candidates have low solubility in water and low bioavailability (Lipinski 2000, 2002; Lipinski et al. 2001). It is known that the dissolution rate and the solubility of a poorly water soluble drug can be improved by milling it into nanoparticles (Filippos et al. 2007; Merisko-Liversidge and Liversidge 2011; Kipp 2004). There are many reports that milling a poorly water soluble drug into nanoparticles increases its bioavailability, reduces food effects, and also has the potential to realize intravenous sustained release (Yuminoki et al. 2014; Jinno et al. 2006; Rabinow 2004). There are two main approaches to prepare nanoparticles (nanoparticles defined here as pure drug crystals, i.e., nanocrystals) of a poorly water soluble drug: "bottom up" and "top down" (Rabinow 2004; Gao et al. 2013). In the "bottom up" approach, a poorly water soluble drug is dissolved in an organic solvent and is precipitated by adding the resulting solution to an aqueous solvent (Ali et al. 2009; de Waard et al. 2008). However, this approach needs an organic solvent to prepare the nanoparticles (Gao et al. 2008). The "top down" approach, which includes media milling and high-pressure homogenization, is more widely used (Merisko-Liversidge and Liversidge 2011; Keck and Müllar 2006). It is based on the size reduction of larger particles through mechanical energy. The "top down" approach can be applied not only to milligram quantities of a drug in the early stage of development, but also to larger amounts of drug in commercial manufacturing (Filippos et al. 2007). However, a conventional stirred beads milling often needs a lot of time to prepare nanoparticles (10 mL suspension, a few hours; 5 L-10 L suspension, 12-48 h) (Filippos et al. 2007). We previously reported nano-milling using a rotation/revolution pulverizer (NP-100) (Takatsuka et al. 2009). This nano-milling, which was one of wet beads millings, was superior to conventional stirred beads milling. This nano-milling could mill phenytoin (0.1 g) into nanoparticles without producing an amorphous state in several min (5 min) by using a smaller amount of zirconia beads (2.4 g) as grinding media. In addition, this nano-milling technology could be applied to other poorly water soluble drugs, and to compounds with low melting points such as beeswax and coenzyme Q_{10} by adjusting the milling conditions (e.g., speed of rotation and revolution, and temperature) (Yuminoki et al. 2012; Onoue et al. 2014). However, the NP-100 is a pulverizer for laboratory scale milling. It is necessary to scale the nano-milling using the rotation/revolution pulverizer up to manufacturing scale. Phenytoin (PHE) was used as a model drug with low solubility in water, and scale up of nano-milling by the rotation/revolution pulverizer from laboratory to manufacturing scale was studied in the present investigation. Before the scaling up study, the oral absorption of PHE was evaluated in animals to verify the improvement of the PHE bioavailability by milling to nanoparticles using the NP-100. Then, the scaling parameters especially the revolution speed, and the drug concentration were evaluated using different sized rotation/revolution pulver-

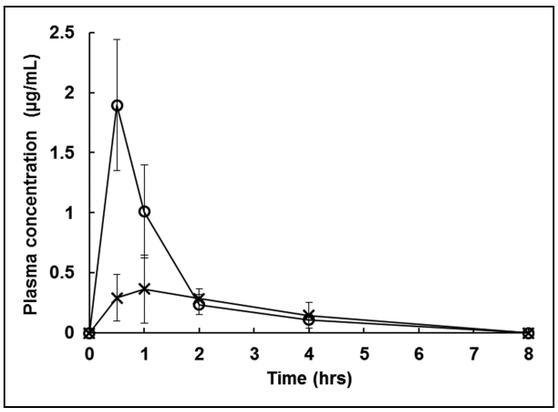

Fig. 1: Plasma concentrations of PHE after oral administration of the original PHE (10 mg/kg) (×) and the milled PHE (10 mg/kg) (◯) to rats. Data represent mean ± SD of 3 independent experiments.

Table 1: Pharmacokinetic parameters of PHE following oral administration to rats

	AUC_{0-8} (μg•hr/mL)	C_{max} (μg/mL)	T_{max} (hr)
Original	1.28 ± 0.34	0.43 ± 0.23	2.33 ± 1.53
milled	2.39 ± 0.28**	1.98 ± 0.46**	0.75 ± 0.29

AUC_{0-8}: area under the curve of blood concentration vs. time from t = 0 to t = 8 hrs after administration; C_{max}: maximum concentration; Tmax: time to maximum concentration. Data represent mean ± SD of 3 determinations.
**, P < 0.01 between the original PHE and the milled PHE.

izers (NP-100, the middle scale model of NP-100 (ARV-3000T) and the large scale model of NP-100 (ARV-10KT)).

2. Investigations, results and discussion

2.1. Pharmacokinetic study of Phenytoin

According to the biopharmaceutics classification system (BCS), PHE is categorized into BCS class II and identified as having low solubility and high membrane permeability (Sarode et al. 2013). The bioavailability of BCS class II compounds is generally limited by their dissolution rate, and is enhanced by increasing their dissolution rate. Niwa et al. (2011) reported that the dissolution rate of PHE was significantly increased by milling it into nanoparticles. Therefore, it was assumed that the oral absorption of PHE would be improved by milling into nanoparticles. We previously reported that the NP-100 could mill PHE (0.1 g) into nanoparticles (D90 = 0.272 μm) without producing an amorphous state (Takatsuka et al. 2009). In the current study, the oral absorption of PHE was evaluated to verify the enhancement of bioavailability of PHE by milling into nanoparticles. Figure 1 shows the plasma concentration-time profile of PHE in rats after oral administration of the original PHE (D90: 36.38 μm) and the milled PHE using the NP-100 (10 mg PHE/kg). Relevant pharmacokinetic parameters including C_{max}, T_{max}, and AUC_{0-8} are listed in Table 1. The milled PHE showed higher exposure than the original PHE, with C_{max} and AUC_{0-8} values of 1.98 ± 0.46 μg/mL and 2.39 ± 0.28 μg•hrs/mL, respectively. The milled PHE showed ca. twofold higher oral bioavailability compared with the original PHE, as well as almost 4.5-fold higher C_{max} ($P < 0.01$).

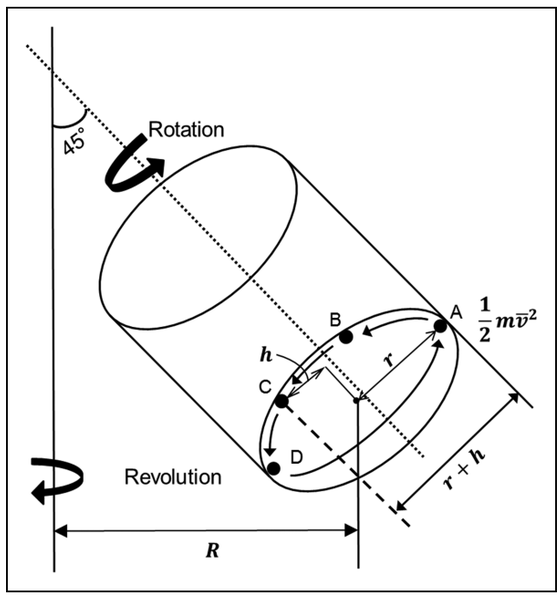

Fig. 2: Movement of beads in the vessel during milling.

2.2. Theoretical and milling scale-up parameters

The NP-100 is a laboratory scale pulverizer. A larger amount of drug is also required for clinical studies and manufacturing. Therefore, the nano-milling must be scaled up. The theory describing milling by the rotation/revolution pulverizer has been reported previously (Takatsuka et al. 2009). Beads in the vessel move continuously due to the rotation of the vessel (like from position A to position D) and beads also move from position D to position A due to the revolution of the vessel (Fig. 2). The drug particles are milled by collision with the beads accelerated by the motion of vessel. Thus, using the equations of uniformly accelerated motion, the mean velocity ($\overline{v}$) of the beads upon collision with the drug particles is described by Eq. (1),

$$\overline{v} = Ggt,\ r + h = \frac{1}{2}Ggt^2 \Rightarrow \overline{v}\sqrt{2Gg(r+h)} \qquad (1)$$

where G is the relative centrifugal acceleration due to revolution (revolution G), g is the gravitational acceleration, t is time which beads are accelerated by revolution G, h is the vertical distance of the beads from the center of the vessel, r is the radius of the rotation. $r + h$ corresponds to the distance by which the beads are accelerated by the revolution G. The revolution G is also described as in Eq. (2),

$$G = 1118 \times 10^{-8} \times R \times N^2 \qquad (2)$$

where R is the radius of the revolution and N is the number of the revolution per minutes (Tanaka et al. 2014). Several reports have described the correlation between the particle size reduction rate of inorganic compounds and the collisional energy of balls during planetary ball milling (Kano et al. 1999; Mio et al. 2002 and 2004). The collisional energy of beads (E_i) during milling could be expressed by beads motion theory as follows (Kano et al. 1999):

$$E_i = \frac{1}{2}\overline{n}m\overline{v}^2 \qquad (3)$$

where $\overline{n}$ and m are defined as the number of collisions of beads with the drug per second, and the mass of a bead, respectively. Kano et al. (1999) also expressed the specific collisional energy

Table 2: Configuration of the three pulverizers

	R (mm)	r (mm)	ω/Ω	The volume of vessel (L)
NP-100	95	35	1.0	0.2
ARV-3000T	248	81.25	0.88	3.1
ARV-10KT	483	109	0.7	12.7

R: Radius of revolution, r: Radius of rotaion (radius of vessel), ω/Ω: Speed ratio of rotaion to revolution.

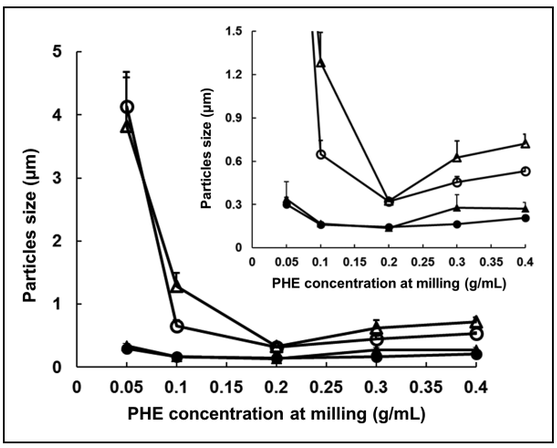

Fig. 3: Effect of PHE concentration on D50 (filled) and D90 (open) values of the milled PHE by using NP-100 (◯) and ARV-3000T (△). Inset is enlarged the area which the particles size of the milled PHE is less than 1.5 μm.

of beads per unit mass of drug (E_w) by transforming Eq. (3) to Eq. (4):

$$E_w = \frac{E_i}{W} = \frac{1}{2W}\overline{n}m\overline{v}^2 \tag{4}$$

where W is the amount of the drug charged in the vessel. However, it is recognized that Eq. (4) is applicable for a dry milling process, whereas nano-milling using the rotation/revolution pulverizer is a wet beads milling process. In wet beads milling, a drug is suspended and milled in solvent (aqueous solution including the stabilizer) and the drug concentration influences the flow properties and the mean velocity of the beads during milling. Thus, it is better to discuss the specific collisional energy using the drug concentration rather than the amount of the drug. The drug concentration (g/mL) was defined as the amount of drug per unit volume of solvent in this study, and the drug concentration (C) was used in Eq. (4) instead of the amount of drug, transforming Eq. (4) to Eq. (5).

$$\Rightarrow E_c = \frac{E_i}{C} = \frac{1}{2C}\overline{n}m\overline{v}^2 \tag{5}$$

E_c is defined the specific collisional energy per unit drug concentration in one second. In addition, Eq. (5) can be expressed as Eq. (6) by using Eq. (1).

$$E_c = \frac{\overline{n}}{c}mGg(r+h) \tag{6}$$

h was provided in a previous report, and expressed here as Eq. 7 (Takatsuka et al. 2009). ω and Ω are defined as the rotation speed and the revolution speed, respectively. So, ω/Ω is the speed ratio of rotation and revolution.

$$h = \frac{R}{\sqrt{2}} - \sqrt{\frac{R^2}{2} - \frac{\omega^2}{\Omega^2} \times 2r^2} \tag{7}$$

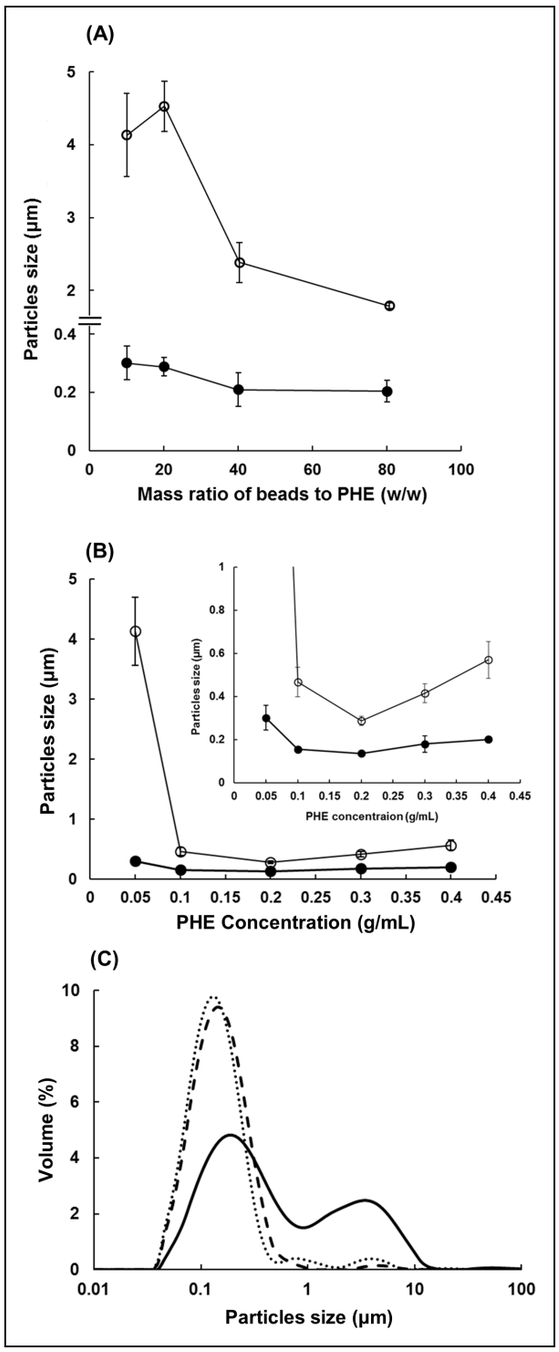

Fig. 4: Effect of the mass ratio of beads to PHE (from 10 to 80) on D50 (filled) and D90 (open) value of the milled PHE (0.25 g) by using NP-100 at the 0.05 g/mL PHE concentration (A). Effect of the PHE concentration (from 0.05 to 0.4 g/mL) on D50 (filled) and D90 (open) value of the milled PHE (0.25 g) by using NP-100 at the 10 mass ratio of beads to PHE (B). Inset in Fig. 4B is enlarged the area which the particles size of the milled PHE is less than 1.0 μm. Particle size distribution (C) of the milled PHE (0.25 g) by using NP-100 under different milling conditions. PHE was milled for 4 min by using 10 mass ratio of beads to PHE and 0.05 g/mL PHE concentration (solid line). PHE was milled for 4 min by using 10 mass ratio of beads to PHE and 0.2 g/mL PHE concentration (dashed line). PHE was milled for 12 min by using 40 mass ratio of beads to PHE and 0.05 g/mL PHE concentration (dotted line).

Table 3: Milling conditions in the optimum PHE concentration study

	PHE Concentration at milling (g/mL)	Bulk size /Batch (g)	Volume of MC solution (mL)	Mass ratio of PHE to beads (w/w) (Beads/PHE)	Revolution speed (rpm)	Time (min)
NP-100	0.05	0.25	5.0	10	2000	4
	0.1	0.5	5.0	10		
	0.2	1.0	5.0	10		
	0.3	1.5	5.0	10		
	0.4	2.0	5.0	10		
ARV-3000T	0.05	5 (2.5 × 2)	100 (50 × 2)	10	750	8
	0.1	10 (5.0 × 2)	100 (50 × 2)	10		
	0.2	20 (10 × 2)	100 (50 × 2)	10		
	0.3	30 (15 × 2)	100 (50 × 2)	10		
	0.4	40 (20 × 2)	100 (50 × 2)	10		

These parameters (R, ω/Ω, and r) were the pulverizer's configurations (Table 2). Therefore, h was a specific parameter for each pulverizer. The gravitational value g was a constant: m was also a constant because the same size beads (ϕ 0.1 mm) were used in this study. It was difficult to calculate $\overline{n}$ accurately, because it was dependent on many parameters (e.g., the mass ratio of beads to drug, the milling time, the rotation and revolution speed, etc.). From the milling mechanism, the mean velocity of beads at collision with drug particles depended on the revolution G (Eq. 1). The revolution G was a controllable parameter, from which the radius and the speed of the revolution could be calculated. The drug concentration related to the flow property of the beads and the viscosity of the drug slurry would influence the collisional energy of the beads. In this study, the revolution G and the drug concentration for the milling process were varied to evaluate the scaling parameters.

2.3. Optimum Phenytoin concentration for milling using a rotation/revolution pulverizer

As shown in Eq. (6), E_c depended on the various parameters including the drug concentration. Several reports have evaluated the effect of a material concentration on milling efficiency using inorganic compounds such as gibbsite and alumina with wet beads milling (Belaroui et al. 1999; Bel Fadhel et al. 2001; He et al. 2004). Therefore, it was important to study the influence of the drug concentration, which is related to E_c, for scaling up nano-milling using the rotation/revolution pulverizer. The PHE concentration was varied from 0.05 g/mL to 0.4 g/mL (Table 3). 0.25 g – 2.0 g PHE was milled in 5 mL aqueous 0.3% (w/v) methylcellulose (MC) solution containing 0.1% (v/v) Tween 80 (MC solution) using the NP-100 and 5.0 g (2.5 g × 2) – 40 g (20 g × 2) PHE was milled in 100 mL (50 mL × 2) MC solution using the ARV-3000T. The beads were added until the mass ratio of beads to PHE was 10. Figure 3 shows the effect of the PHE concentration on the particles size distribution of the milled PHE by the NP-100 and the ARV-3000T. The particles size of the milled PHE decreased with an increase in the PHE concentration up to 0.2 g/mL, but the particles size at PHE concentrations of 0.3 g/mL and 0.4 g/mL were slightly larger than at 0.2 g/mL. The results using the ARV-3000T were similar to the NP-100. According to Eq. (6), E_c decreased with an increase in the PHE concentration. The viscosity of the PHE slurry during milling increased with an increase in the PHE concentration and the flow property of beads was lower. Thus, beads in the vessel had less collisional energy to mill PHE into fine nanoparticles efficiently at PHE concentrations over 0.3 g/mL. On the other hand, the experimental results for PHE concentrations of less than 0.1 g/mL were different from the anticipation from Eq. (6). The differences between the experimental and the anticipation from Eq. (6) may be due to the influence of $\overline{n} \cdot \overline{n}$ increased with an increase in PHE, because the number of PHE particles in the solvent increased. In order to verify the effect of, the effect of $\overline{n}$; the mass ratio of beads to PHE on the particles size distribution of the milled PHE (0.25 g) was evaluated at a PHE concentration of 0.05 g/mL by using the NP-100 (Fig. 4A). In addition, the effect of the PHE concentration on the particles size distribution of the milled PHE (0.25 g) was evaluated at a mass ratio of beads to PHE of 10 by using the NP-100 (Fig. 4B). These experimental conditions are listed in Table 4. Figure 4A shows that the particles size of the milled PHE decreased with increasing mass ratio of beads to PHE. However, the D90 value of the milled PHE was never less than 1 μm. Fig. 4B shows that 0.25 g PHE could be milled into nanoparticles at PHE concentrations above 0.1 g/mL at mass ratio of beads to PHE of 10. The particles size of the milled PHE was the smallest at 0.2 g/mL of the PHE concentration. 0.25 g PHE could also be milled to nanoparticles (D90 = 0.273 μm) at a PHE concentration of 0.05 g/mL, when the mass ratio of beads to PHE and the milling time were 40 and 12 min, respectively (Fig. 4C). Therefore, the higher mass ratio of beads to PHE and longer milling time were necessary to mill PHE at the 0.05 g /mL of PHE concentration. It was expected that the E_c at the lower PHE concentration was lower than at the higher PHE concentration, because $\overline{n}$ in Eq. (6) was smaller. The general solution to obtain more $\overline{n}$ was to increase the mass ratio of beads to PHE. A longer milling process was also needed to obtain fine nanoparticles at lower E_c. However, it is undesirable to increase the milling time and the mass ratio of beads to PHE for scaling up nano-milling. Specifically, using a higher mass ratio of beads to PHE increases contamination and gross weight, both of which impose a burden on the machine. In addition, from Figs. 3 and 4, the drug concentration was found to be a more important parameter than the milling time or the mass ratio to obtain higher $\overline{n}$. The surface area of PHE in the solvent was larger than that of the beads, because the particle size and the density of PHE was smaller than that of the beads. Increasing the PHE concentration to increase $\overline{n}$ was effective because the probability of collision between beads and PHE was enhanced by increasing the surface area of PHE. Therefore, the drug concentration was an essential parameter for milling PHE into nanoparticles effectively and for scaling up the nano-milling. The drug concentration at which PHE could be efficiently milled to nanoparticles was determined to be 0.2 g/mL.

2.4. Effect of the revolution G on the particle size distribution of Phenytoin milled by NP-100 and ARV-3000T

The NP-100, with a small rotation and revolution radius, needed a high rotation/revolution speed to provide enough collisional

Table 4: Milling condition in the effect of $\bar{n}$ study

	Bulk size /Batch (g)	Mass ratio of PHE to beads (w/w) (Beads/PHE)	Volume of MC solution (mL)	PHE Concentration at milling (g/mL)	Revolution speed (rpm)	Time (min)
NP-100	0.25	10	5.0	0.05	2000	4
		20	5.0	0.05		
		40	5.0	0.05		
		80	5.0	0.05		
		10	2.5	0.1		
		10	1.25	0.2		
		10	0.833	0.3		
		10	0.625	0.4		

Table 5: Milling conditions in the study of the correlation between NP-100 and ARV-3000T

	Bulk size (g) /Batch	Zirconia Beads (g)	PHE Concentration at milling (g/mL)	Revolution G (G) (revolution speed)	Time (min)
NP-100	1.0	5.0	0.2	185 (1320 rpm)	20
	1.0	5.0	0.2	145 (1160 rpm)	20
	1.0	5.0	0.2	107 (1000 rpm)	20
ARV-3000T	200 (100 × 2)	1000 (500 × 2)	0.2	185 (850 rpm)	20
	200 (100 × 2)	1000 (500 × 2)	0.2	145 (750 rpm)	20
	200 (100 × 2)	1000 (500 × 2)	0.2	107 (650 rpm)	20

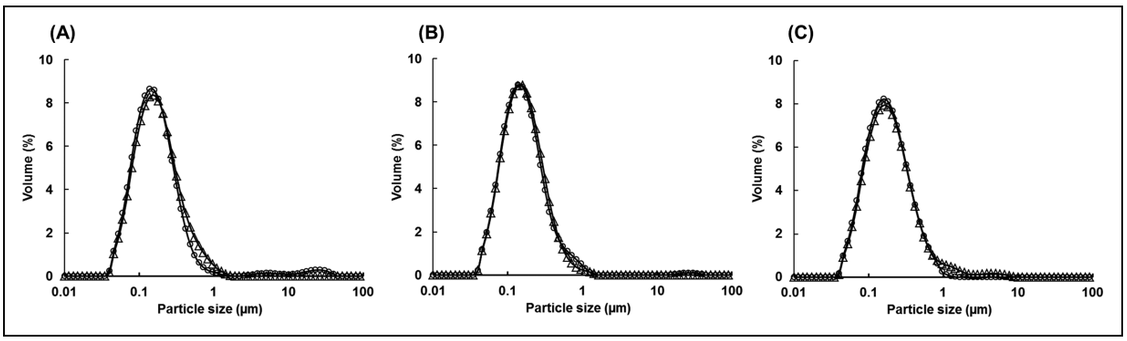

Fig. 5: Effect of the revolution G [185 G (A), 145 G (B), and 107 G (C)] on the particle size distribution of the milled PHE by NP-100 (◯) and ARV-3000T (△).

energy to mill the nanoparticles. On the other hand, the ARV-3000T and the ARV-10KT could provide enough collisional energy at a lower rotation/revolution speed than the NP-100, because they had a larger radius of rotation and revolution than the NP-100. In this section, the effect of the revolution G which was calculated by the radius and the speed of the revolution on the particle size distribution of the milled PHE by using the NP-100 and the ARV-3000T was evaluated. The experimental milling conditions are shown in Table 5. It was assumed from Eq. (6) that E_c could be controlled by adjusting the revolution G and the drug concentration. The PHE concentration and the mass ratio of beads to PHE were 0.2 g/mL and 5, respectively. One gram and 100 g PHE were milled for 20 min in the NP-100 and the ARV-3000T, respectively. The revolution G was varied from 107 to 185 (speeds for each mill calculated from Eq. (2), and detailed in Table 5). Figure 5 shows the particle size distribution of the milled PHE using the NP-100 and the ARV-3000T. The particle size distribution of the milled PHE by the ARV-3000T was similar to that of the milled PHE by the NP-100 at each of the three discrete revolution G conditions. The ARV-3000T had good correlation with the NP-100 when the revolution G and the PHE concentration were the same. It was assumed that almost the same E_c was obtained at the same drug concentration and the same revolution G from Fig. 5 and Eq. 6.

2.5. Scaling up of Phenytoin bulk size from milligram to kilogram scale

The revolution G and the PHE concentration were important parameters to scale up nano-milling using the rotation/revolution pulverizer. Using these parameters to mill PHE into nanoparticles, the scaling up of PHE bulk size was evaluated using the ARV-3000T and the ARV-10KT using milling conditions at which the revolution G and the PHE concentration were 145 G and 0.2 g/mL, respectively (Table 6). The PHE bulk size was chosen by considering the volume of the vessel. Additionally, a smaller mass ratio of beads to PHE was used for the ARV-3000T and the ARV-10KT (5 and 3 ratios, respectively) compared with the NP-100 (25 ratio), because too large of a mass ratio of beads to PHE caused a decrease in the speeds of rotation and revolution during milling due to overloading. Figure 6 shows the plot of the D50 and D90 values of the milled PHE by using the ARV-3000T and the ARV-10KT at each milling time. The D50 and D90 values of the milled PHE by the ARV-3000T and the ARV-10KT decreased as milling time proceeds and became almost constant over 30 min and 60 min, respectively. The ARV-3000T could mill 500 g (250 g × 2) PHE to nanoparticles (D90 = 0.295 μm) in 30 min. The ARV-10KT could mill 2,000 g (1,000 g × 2) PHE to nanoparticles (D90 = 0.316 μm) in ca. 60 min (Fig. 7A and Table 7). In addition, the particle size distribution of the milled

Table 6: Milling conditions using the ARV-3000T and the ARV-10KT in the PHE bulk study

	Bulk size (g) /Batch	Zirconia Beads (g)	PHE Concentration at milling (g/mL)	Revolution G (G) (revolution speed)	Time (min)
NP-100	0.1	2.5	0.2	145 (1160 rpm)	6
ARV-3000T	500 (250 × 2)	2,500 (1,250 × 2)	0.2	145 (750 rpm)	5-35
ARV-10KT	2,000 (1,000 × 2)	6,000 (3,000 × 2)	0.2	145 (520 rpm)	10-70

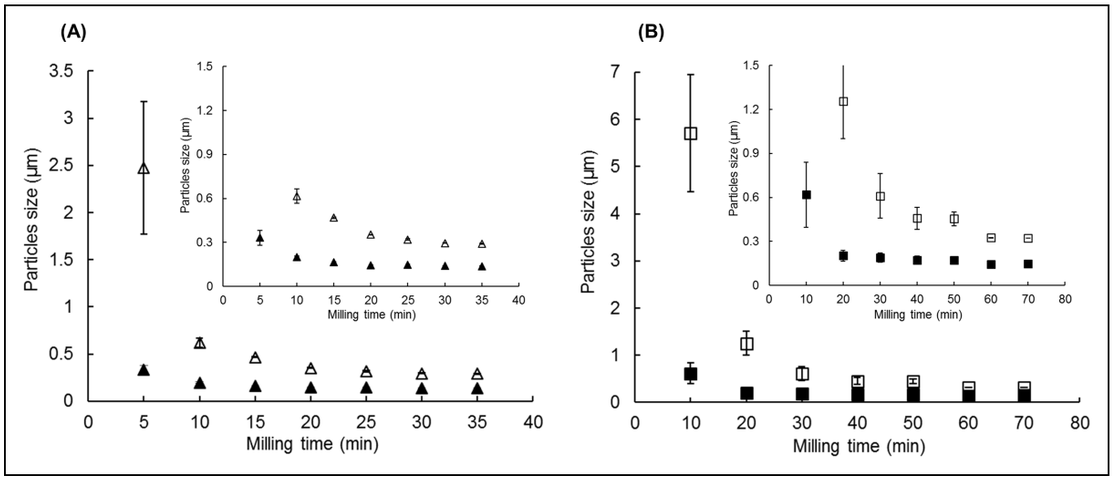

Fig. 6: Effect of the milling time on D50 (filled) and D90 (open) value of the milled PHE by using ARV-3000T (A) and ARV-10KT (B). Inset is enlarged the area which the particles size of the milled PHE is less than 1.5 μm.

Table 7: Particle size distribution (D10, D50 and D90 value) of the milled PHE by three pulverizers

	D10 (μm)	D50 (μm)	D90 (μm)
Original phenytoin	11.50 ± 0.050	20.88 ± 0.140	36.38 ± 0.343
Milled phenytoin			
NP-100 (0.1 g)	0.069 ± 0.023	0.144 ± 0.002	0.317 ± 0.003
ARV-3000T (250 g × 2)	0.065 ± 0.001	0.139 ± 0.001	0.295 ± 0.002
ARV-10KT (1,000 g × 2)	0.069 ± 0.002	0.143 ± 0.006	0.312 ± 0.009

PHE by the ARV-3000T and the ARV-10KT was almost the same as that of the milled PHE by the NP-100. The milled PHE powders using the ARV-3000T and the ARV-10KT was analyzed by SEM to check their morphology (Fig. 7B). From these SEM images, nano-sized PHE particles were confirmed. The milled PHE powders were analyzed by using PXRD and DSC to evaluate their crystallinity (Fig. 8). The PXRD patterns of each milled PHE powder were equal to that of original PHE and halo patterns (i.e. amorphous form) were not detected. Additionally, the melting point of each milled PHE powder was the same as that of original PHE and other exothermic and endothermic peaks were not detected by DSC. From PXRD and DSC, the crystallinity of the milled PHE using the ARV-3000T and the ARV-10KT was maintained and amorphous phase was not detected.

2.6. Conclusions

In this study, the oral absorption of PHE was improved by milling into nanoparticles with the NP-100. The scaling parameters of the rotation/revolution pulverizer were evaluated. The revolution G, which was calculated by the revolution radius and speed, and the drug concentration in the suspension were shown to be the two most important parameters of the nano-milling process. As a result, the ARV-3000T had good correlation with the NP-100 when revolution G and the PHE concentration at milling were the same. Additionally, using these same parameters, the rotation/revolution pulverizer could mill 2,000 g (1,000 g × 2) of PHE to nanoparticles in 60 min, which is a shorter milling time than that of a conventional stirred media milling in the manufacturing stage. The milled PHE by the ARV-3000T and the ARV-10KT maintained its crystallinity, and no amorphous phase was detected by PXRD and DSC. The rotation/revolution pulverizer could prepare nanoparticles with identical physical properties from the milligram scale to the kilogram scale. It is possible to predict the milling condition of the kilogram scale from the milling condition of the milligram scale by using knowledge of the scaling up parameters of the rotation/revolution pulverizer. Therefore, this work suggest nano-milling by using rotation/revolution pulverizer will be widely applicable to the development of nano-medicine.

3. Experimental

3.1. Materials

Phenytoin (PHE) was purchased from Shizuoka Coffein Co., Ltd. (Shizuoka, Japan). Methylcellulose (MC) (Metolose SM-4000) and Tween 80 (polysorbate 80) were purchased from Shin-Etsu Co., Ltd. (Tokyo, Japan) and Wako Pure Chemical Industries Co., Ltd. (Osaka, Japan), respectively. Zirconia (zirconium oxide) beads (hereafter called 'beads') with median diameter of 0.1 mm (the range of particles size: 0.08 – 0.13 mm)) were purchased from

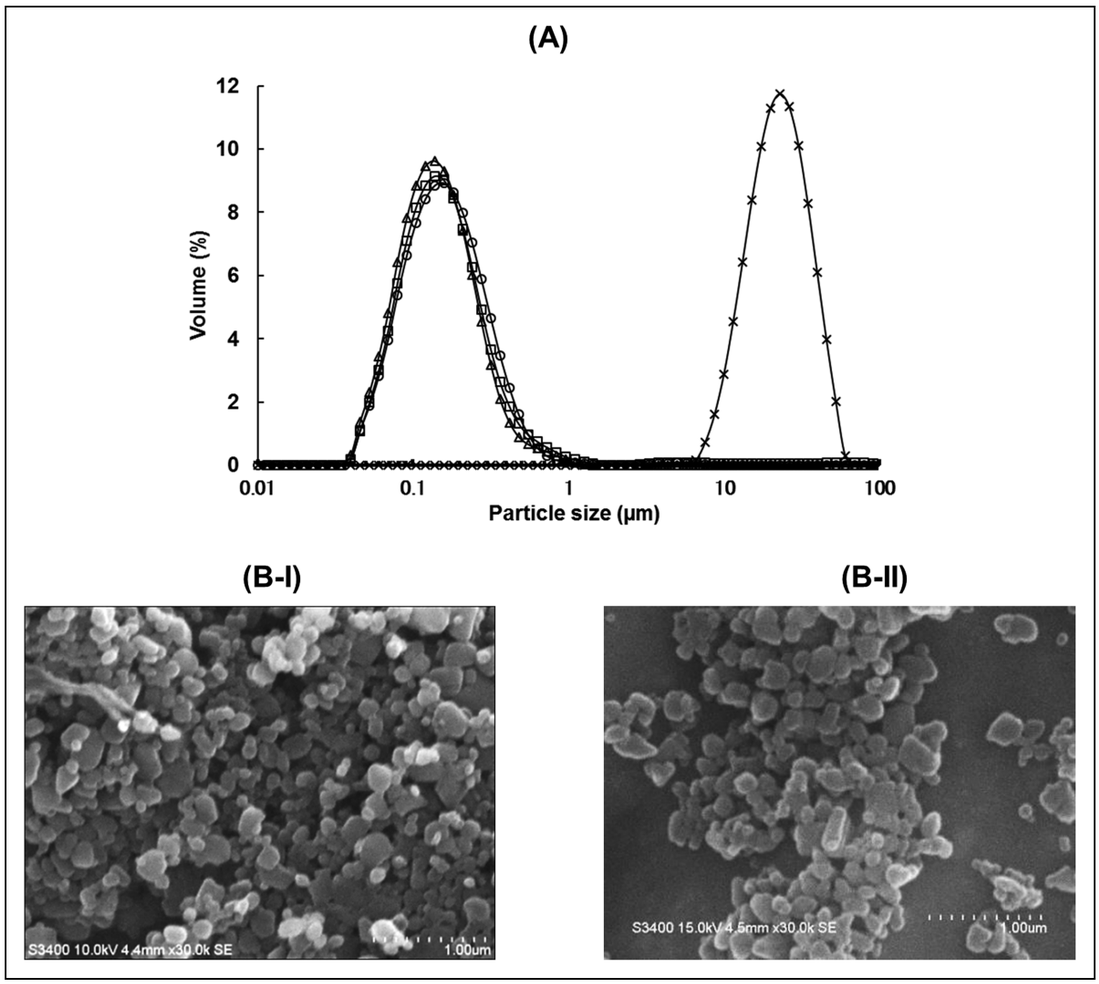

Fig. 7: Particle size distribution (A) of the original PHE (×), the milled PHE by using NP-100 (◯), ARV-3000T (Δ), and ARV-10KT (□) and SEM micrographs (B) of the milled PHE by ARV-3000T (B-I) and ARV-10KT (B-II).

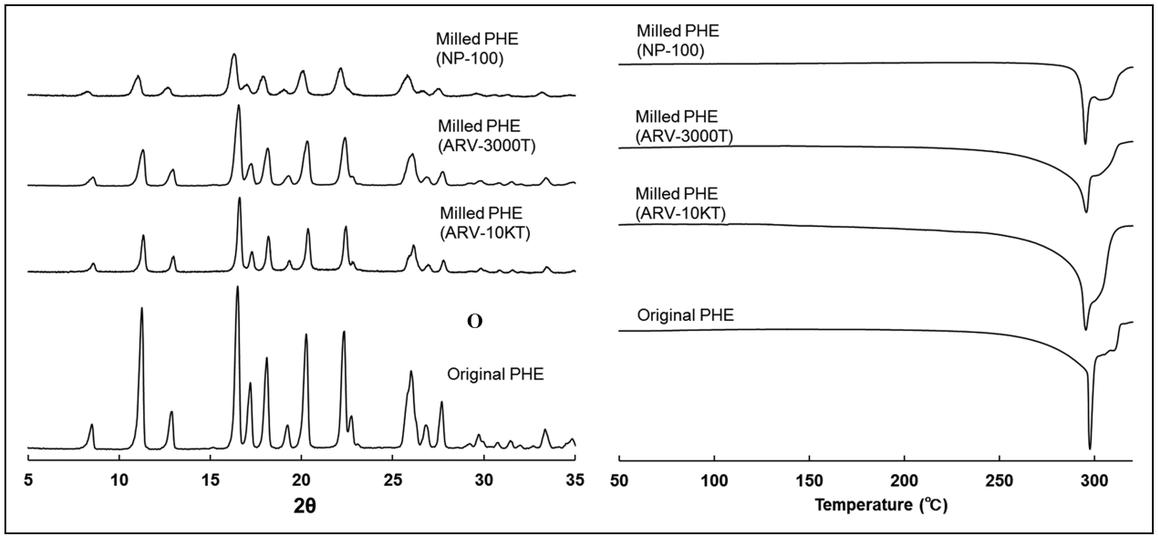

Fig. 8: PXRD patterns (A) and DSC thermographs (B) of the original PHE and the milled PHE by using NP-100, ARV-3000T, and ARV-10KT.

Nikkato Co., Ltd. (Osaka, Japan). All other reagents were analytical-grade commercial products.

3.2. Preparation of Phenytoin nano-suspension by rotation/revolution pulverizer

We previously reported the method for preparing a PHE nano-suspension using a rotation/revolution pulverizer (NP-100, Thinky Corp., Tokyo, Japan) (Takatsuka et al 2009). PHE was weighed into the NP-100 zirconia vessel (hereafter called 'vessel') and beads and an appropriate volume of an aqueous polymer solution were added. In this study, aqueous 0.3% (w/v) MC solution containing 0.1% (v/v) Tween 80 (hereafter called 'MC solution') was used as the aqueous polymer solution. Preparation of the PHE nano-suspension involved two processes: (1) the milling process and (2) the dispersion process. In the milling process, the particle size of PHE was decreased to nanoparticles. In the dispersion process, the milled PHE was dispersed in the MC solution to separate beads from the PHE suspension and the concentration of PHE suspension was adjusted. The middle scale model of NP-100 (ARV-3000T, Thinky Corp., Tokyo, Japan) and the large scale model of NP-100 (ARV-10KT, Thinky Corp., Tokyo, Japan) were used to scale up the nano-milling (Table 2). Unlike NP-100, ARV-3000T and ARV-10KT consisted of two vessels. The speed ratio of rotation to revolution which ARV-3000T and ARV-10KT had was 0.88 and 0.7, respectively. The procedure for preparing the PHE nano-suspension using ARV-3000T and ARV-10KT was the same as for the NP-100. The milled PHE powders were prepared by freeze-drying the suspension of the milled PHE in order to analyze PHE morphology and crystallinity. The suspension of the milled PHE was frozen with liquid nitrogen and freeze-dried using the FD-81 freeze-dryer (Tokyo Rikakikai, Tokyo, Japan, trap chilling temperature -75 °C, 10 Pa) for 48 h.

3.3. Particle size distribution measurement

The nano-suspensions of the milled PHE were diluted to approximately 10 mg/mL with MC solution and sonicated for 5 min. The particle size distribution of the milled PHE was analyzed using a laser diffractometer (Mastersizer 2000, Malvern Instruments, WR, UK) with a small-volume dispersing unit (Hydro 2000 μP, Malvern Instruments). The particle size distribution was based on volume and was expressed in terms of the diameters at 50% (D50) and 90% (D90) of the population distribution.

3.4. Particle morphology measurement

A scanning electron microscope (SEM) (S-3400, Hitachi High-Technologies Co., Ltd., Tokyo, Japan) operating at 10-15 keV was used to analyze the morphology of the milled PHE powders prepared with the ARV-3000T and the ARV-10KT. Prior to SEM analysis, each powder was dispersed onto a carbon-tape-coated aluminum stub and then sputtered with gold.

3.5. Powder X-ray diffraction (PXRD)

PXRD patterns of the original PHE powder and the milled PHE powder were obtained using a RINT model (Rigaku Corp., Tokyo, Japan) instrument with Cu radiation generated at 40 mA and 40 kV. Data were obtained from 5 to 35 ° (2θ) at a step rate of 0.02 °and a scanning speed of 2 °/min.

3.6. Differential scanning calorimetry (DSC)

DSC was performed using a DTG-60 model (Shimadzu Corporation, Kyoto, Japan) instrument. DSC data were obtained in an open aluminum pan using approximately 8 mg of sample (the original PHE powder or the milled PHE powder) and approximately 7 mg of alumina as the reference material. The sample was heated from 50 to 320 °C at a heating rate of 5 °C/min with a 50 mL/min nitrogen purge.

3.7. High performance liquid chromatography (HPLC) analysis

HPLC system (Hitachi High-Technologies Corp., Tokyo, Japan) equipped with a L-7200 auto-injector, a L-7100 solvent delivery pump, a L-7610 degasser, and a L-7455 photodiode array detector (DAD) at a detection wavelength of 195 nm was used. The column was a ZORBAX XRB-C18 (particle size: 5.0 μm; column size: I.D. 2.1 mm × 50 mm; Agilent Technologies, Inc., CA, US); the column temperature was maintained at 30 °C. The mobile phase consisted of 20 mM sodium dihydrogen phosphate aqueous solution – acetonitrile [75:25 (v/v)] and the flow rate was 0.3 mL/min.

3.8. Pharmacokinetic study

4.8.1. Preparation condition of Phenytoin nanosuspension by the NP-100 for pharmacokinetic study

The milled PHE nanosuspension was prepared by the milling condition in our previous report (Takatsuka et al. 2009). PHE (0.1 g) and beads (2.5 g) was weighed into the vessel and milled at 2000 rpm for 2 min by the NP-100 with MC solution. After that, 9.5 mL of the MC solution was added and milled at 400 rpm for 1 min to disperse the milled PHE in MC solution. The final concentration of PHE nanosuspension was 10 mg/mL.

3.8.1. Animals and drug administration

Male Sprague-Dawley rats (Japan SLC, Shizuoka, Japan), weighing 281 ± 9.47 g, were housed three per cage in the laboratory with free access to food and water, and maintained on a 12 h dark/light cycle at controlled temperature (24 ± 1 °C) and humidity (55 ± 5%). All the procedures used in the present study were conducted according to the guidelines approved by the Institutional Animal Care and Ethical Committee of Setsunan University. The pharmacokinetics of the original PHE and the PHE milled using the NP-100 were studied. For oral administration, the original PHE were suspended in water at 10 mg/mL. 10 mg/mL milled PHE suspension was prepared by using the NP-100. Rats were fasted for 18 h before being orally treated with the original PHE and the milled PHE suspension by oral gavage (10 mg PHE/kg).

3.8.2. Plasma concentration of Phenytoin

Blood samples (200 μL) were taken from the cannulated jugular vein at 0.5, 1.0, 2.0, 4.0 and 8.0 h after oral administration. The blood samples were centrifuged at 2,330 × *g* for 5 min (4 °C) to prepare plasma samples, then the plasma samples (75 μL) were mixed with acetonitrile (75 μL) and centrifuged at 12,100 × *g* for 5 min. The supernatants were collected in a glass tube and kept frozen at -80 °C until analysis. The plasma concentration of PHE was determined by HPLC-DAD as described in the "HPLC analysis" section. The pharmacokinetic parameters for PHE were calculated by 1-compartmental methods using the Gastroplus® program (Ver. 8.5, Simulations Plus, Inc., CA, US).

3.9. Statistical analysis

The p-values of the pharmacokinetic parameters were calculated using the F-test and T-test. Values less than 0.05 were considered significant.

References

Ali HSM, York P, Blagden N (2009) Preparation of hydrocortisone nanosuspension through a bottom–up nanoprecipitation technique using microfluidic reactors. Int J Pharm 375:107–113.

Belaroui K, Pons MN, Vivier H, Meijer M (1999) Wet grinding of gibbsite in a bead-milling. Powder Technol. 105: 396–405.

Bel Fadhel H, Frances C (2001) Wet batch grinding of alumina hydrate in a stirred bead mill. Powder Technol 119: 257–268.

de Waard H, Hinrichs WL, Frijlink HW (2008) A novel bottom–up process to produce drug nanocrystals: controlled crystallization during freeze-drying. J Control Release 128:179–183.

Filippos K, Santipharp P, Yunhui W (2007) Nanosizing-oral formulation development and biopharmaceutical evaluation. Adv Drug Deliv Rev 59: 631–644.

Gao L, Liu G, Ma J, Wang X, Zhou L, Li X, Wang F (2013) Application of drug nanocrystal technologies on oral drug delivery of poorly soluble drugs. Pharm Res 30: 307–324.

Gao L, Zhang D, Chen M (2008) Drug nanocrystals for the formulation of poorly water soluble drugs and its application as a potential drug delivery system. J Nanopart Res 10: 845–62.

He M, Wang Y, Forssberg E (2004) Slurry rheology in wet ultrafine grinding of industrial minerals: a review. Powder Technol 147: 94–112.

Jinno J, Kamada N, Miyake M, Yamada K, Mukai T, Odomi M, Toguchi H, Liversidge GG, Higaki K, Kimura T (2006) Effect of particle size reduction on dissolution and oral absorption of a poorly water soluble drug, cilostazol, in beagle dogs. J Control Release 111: 56–64.

Kano J, Mio H, Saito F (1999) Correlation of size reduction rate of inorganic materials with impact energy of ball in planetary ball milling. J Chem Engin Japan 32: 333–342.

Keck CM. Müller RH (2006) Drug nanocrystals of poorly soluble drugs produced by high pressure homogenization. Eur J Pharm Biopharm 62: 3–16.

Kipp JE (2004) The role of solid nanoparticles technology in the parenteral delivery of poorly water soluble drugs. Int J Pharm 284:109–122.

Lipinski CA (2000) Drug-like properties and the causes of poor solubility and poor permeability. J Pharmacol Toxicol Methods 44: 235–249.

Lipinski CA, Lombardo F, Dominy BW, Feeney PJ (2001) Experimental and computational approaches to estimate solubility and permeability in drug discovery and development settings. Adv Drug Deliv Rev 46: 3–26.

Lipinski CA (2002) Poor aqueous solubility – an industry wide problem in drug discovery. Am Pharm Rev 5: 82–85.

Merisko-Liversidge E, Liversidge GG (2011) Nanosizing for oral and parenteral drug delivery: A perspective on formulating poorly water soluble compounds using wet media milling technology. Adv Drug Deliv Rev 63: 427–440.

Mio H, Kano J, Saito F (2004) Scale-up method of planetary ball mill. Chem Engin Sci 59: 5909–5916.

Mio H, Kano J, Saito F, Kaneko K (2002) Effect of rotational direction and rotaion-to-revolution speed ratio in planetary ball milling. Materials Science and Engineering A332: 75–80.

Niwa T, Miura S, Danjo K (2011) Design of dry nanosuspension with highly spontaneous dispersible characteristics to develop solubilized formulation for poorly water-soluble drugs. Pharm Res 28: 2339–49.

Onoue S, Takahashi H, Kawabata Y, Seto Y, Hatanaka J, Timmermann B, Yamada S (2010) Formulation design and photochemical studies on nanocrystal solid dispersion of crucumin with improved oral bioavailability. J Pharm Sci 99: 1871–1881.

Onoue S, Terasawa N, Nakamura T, Yuminoki K, Hashimoto N, Yamada S (2014) Biopharmaceutical characterization of nanocrystalline solid dispersion of coenzyme Q10 prepared with cold wet-milling system. Eur J Pharm Sci 53: 118–125.

Rabinow BE (2004) Nanosuspensions in drug delivery. Nat Rev Drug Discov 3: 785–796.

Sarode A, Wang P, Cote C, Worthen DR (2013) Low-viscosity hydroxypropylcellulose (HPC) grades SL and SSL: versatile pharmaceutical polymers for dissolution enhancement, controlled release, and pharmaceutical processing. AAPS Pharm Sci Tech 14: 151–159.

Takatsuka T, Endo T, Jianguo Y, Yuminoki K, Hashimoto N (2009) Nanosizing of poorly water soluble compounds using rotation/revolution mixer. Chem Pharm Bull 57: 1061–1067.

Tanaka Y, Ueyama H, Ogata M, Daikoku T, Morimoto M, Kitagawa A, Imajo Y, Tahara T, Inkyo M, Yamaguchi N, Nagata S (2014) Evaluation of nanodispersion of iron oxides using various polymers. Indian J Pharm Sci 76: 54–61.

Yuminoki K, Seko F, Horii S, Takeuchi H, Teramoto K, Nakada Y, Hashimoto N (2014) Preparation and evaluation of high dispersion stable nanocrystal formulation of poorly water-soluble compounds by using povacoat. J Pharm Sci 103: 3772–3781.

Yuminoki K, Takeda M, Kitamura K, Numata S, Kimura K, Takatsuka T, Hashimoto N (2012) Nanopulverization of poorly water soluble compounds with low melting points by a rotation/revolution pulverizer. Pharmazie 67: 681–686.